JOC Article

Hexameric and Pentameric Slipped-Cofacial Dimers: Toward an Artificial Light-Harvesting Complex

Ryoichi Takahashi[†] and Yoshiaki Kobuke*[,†,‡]

Graduate School of Materials Science, Nara Institute of Science and Technology, and CREST, Japan Science and Technology Corporation (JST), 8916-5 Takayama, Ikoma, Nara 630-0192, Japan

kobuke@ms.naist.jp

Received November 23, 2004

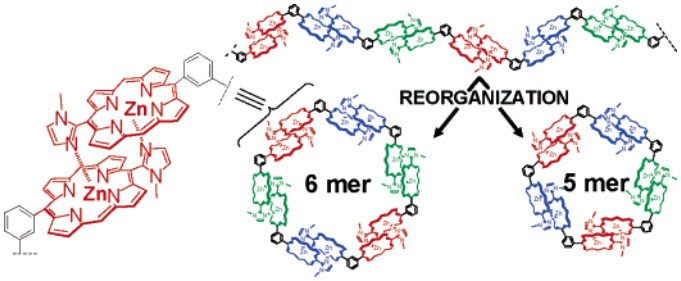

We prepared a zinc complex of bis(1-methylimidazolyl)-*m*-gable porphyrin. The automatically assembled coordinate species showed a complex mixture of wide molecular weight distributions accompanied with assemblies of specific assembly numbers. When this zinc complex was once dissociated by the addition of methanol and reorganized again by elimination of the methanol under high-dilution conditions in chloroform to facilitate intramolecular coordinate structure formation, two convergent assemblies were obtained through analysis by gel permeation chromatography. These assemblies gave round-shaped particles on solid substrates by probe microscopies (atomic force and scanning tunneling microscopies). These two components were separated by GPC and evidence from small-angle X-ray scattering measurements in solution with synchrotron radiation was consistent with hexameric and pentameric macrorings of the gable porphyrin. The porphyrin macrorings did not show any fluorescence quenching by assembly formation, and we anticipate that the macrorings of gable porphyrins represent a good model for an artificial light-harvesting complex.

Introduction

The first event of a photosynthetic reaction is the absorption of light by light-harvesting antenna complexes arranged around the reaction center complex. The structures of light-harvesting antenna systems for LH1, LH2, and LH3 complexes of photosynthetic purple bacteria have been determined by X-ray crystallographies[1] and electron microscopies.[2] In these complexes, 32 bacteriochlorophylls in LH1 and 18 or 16 ones in B850 of LH2 are arranged in macroring structures with use of bacteriochlorophyll-*a* dimers, which are characterized as being in slipped-cofacial orientations to each other. These macrorings are believed to be associated with the most important function in light harvesting. Therefore, structural arrangement of porphyrins into a macroring is extremely interesting for elucidating the mechanism of highly efficient excitation energy transfer and developing useful light-harvesting systems. Until now several oligomeric porphyrins, particularly in circular forms, have been synthesized through both covalent[3] and supramolecular[3b,4] approaches toward light-harvesting antenna mimics. However, there are no systematic studies that would allow a rational design of self-assembled macrorings with the desired properties toward antenna function. To the best of our knowledge, there was no example of a porphyrin macroring composed of self-assembled dimer units.

[†] Nara Institute of Science and Technology (NAIST).
[‡] CREST, Japan Science and Technology Corporation (JST).

(1) (a) McDermott, G.; Prince, S. M.; Freer, A. A.; Hawthornthwaite-Lawless, A. M.; Papiz, M. Z.; Cogdell, R. J.; Isaacs, N. W. *Nature* **1995**, *374*, 517−521. (b) Koepke, J.; Hu, X.; Muenke, C.; Schulten, K.; Michel, H. *Structure* **1996**, *4*, 581−597. (c) McLuskey, K.; Prince, S. M.; Cogdell, R. J.; Isaacs, N. W. *Biochemistry* **2001**, *40*, 8783−8789.

(2) (a) Karrasch, S.; Bullough, P. A.; Ghosh, R. *EMBO J.* **1995**, *14*, 631−638. (b) Savage, H.; Cyrklaff, M.; Montoya, G.; Kühlbrandt, W.; Sinning, I. *Structure* **1996**, *4*, 243−252. (c) Walz, T.; Jamieson, S. J.; Bowers, C. M.; Bullough, P. A.; Hunter, C. N. *J. Mol. Biol.* **1998**, *282*, 833−845.

10.1021/jo047923n CCC: $30.25
Published on Web 03/01/2005

In preceding reports, we introduced an idea to organize slipped-cofacial porphyrin dimers into macrorings to construct an artificial light-harvesting complex of the LHs of photosynthetic purple bacteria, in a hope to unveil the function of this unique cyclic structure.[5] Bis(1-methylimidazolyl)porphyrin dimer, free base **1** and its zinc complex **2**, was employed as the basic structural unit (Scheme 1).

The critical point of this molecular unit is the introduction of two 1-methylimidazolyl groups at the opposite ends of the porphyrins connected by a *m*-phenylene bridge. This molecular design should provide two important characteristics for constructing the supramolecular antenna model. First, the complementary coordination between imidazolyl and central zinc ion is further facilitated by $\pi-\pi$ stacking interaction between porphyrin rings and characterized by a large association constant ($K_a > 10^{10}$ M^{-1}).[6,7] The resulting supramolecule shows a large splitting of Soret band through exciton coupling interaction of two porphyrins in a slipped-cofacial arrangement in a close distance. Therefore, it satisfies perfectly the functional requisites of the light-harvesting dimer unit, in terms of the distance and the orientation of chromophores for favorable energy transfer without quenching of excitation energy. Second, the ring structure will be provided by connecting two mono(imidazolyl)porphyrinatozinc(II) with a 1,3-phenylene spacer, a so-called "gable porphyrin".[8] In contrast to the *meso*-*meso*-coupled bis(1-methylimidazolyl)porphyrinatozinc(II), which grows linearly into a giant porphyrin array reflecting the large association constant,[7] the spatial orientation of 120° is expected to give a closed ring under appropriate conditions. If all of these designs work perfectly, a dodecaporphyrin array composed of hexakis(gable porphyrin) **3** would be constructed. This porphyrin macroring array should have a barrel structure with center-to-center distances of 6.1 and 11.0 Å, in close analogy to those of the light-harvesting complexes of photosynthetic purple bacteria. The remaining four *meso*-positions are substituted by alkyl or olefinic groups to give the assembly reasonable solubility in organic solvents or further functionalization such as covalent connection of the complementary coordination pair.[5b,c]

SCHEME 1. Molecular Design for Formation of Supramolecular Macrocycle 3 by Complementary Coordination of Bis(1-methylimidazol-2-yl) Gable Porphyrinnatozinc(II) 2 from Its Free Base 1[a]

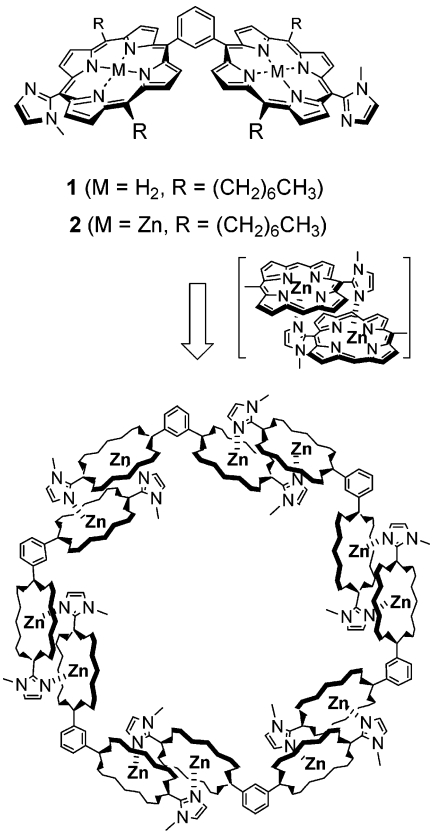

[a] *meso*-Substituents of coordinated species are abbreviated for clarity for **3**.

Results and Discussion

Preparation and Characterization of Gable Porphyrin. In preliminary experiments, we prepared several dipyrromethane derivatives and the corresponding porphyrins with candidates of alkyl and aryl *meso*-substituents. These surveys in the preparations are discussed in Supporting Information. Finally, we utilized *m*-(*n*-heptyl)dipyrromethane[9] and succeeded in the synthesis of bis(imidazolyl)-substituted gable porphyrin **1** with consideration of the previous knowledge to overcome the scrambling reactions of *meso*-substituents (see Support-

(3) (a) Sanders, J. K. M. In *Comprehensive Supramolecular Chemistry*; Atwood, J. L., Davies, J. E. D., MacNicol, D. D., Vögtle, F., Eds.; Pergamon Press: Oxford, 1996; Vol. 9, pp 131−164. (b) Sanders, J. K. M. In *The Porphyrin Handbook*; Kadish, K. M., Smith, K. M., Guilard, R., Eds.; Academic Press: New York, 2000; Vol. 3, pp 347−368. (c) Anderson, S.; Anderson, H. L.; Bashall, A.; McPartlin, M.; Sanders, J. K. M. *Angew. Chem., Int. Ed. Engl.* **1995**, *34*, 1096−1099. (d) Biemans, H. A. M.; Rowan, A. E.; Verhoeven, A.; Vanoppen, P.; Latterini, L.; Foekema, J.; Schenning, A. P. H. J.; Meijer, E. W.; de Schryver, F. C.; Nolte, R. J. M. *J. Am. Chem. Soc*. **1998**, *120*, 11054−11060. (e) Li, J.; Ambroise, A.; Yang, S. I.; Diers, J. R.; Seth, J.; Wack, C. R.; Bocian, D. F.; Holten, D.; Lindsey, J. S. *J. Am. Chem. Soc.* **1999**, *121*, 8927−8940. (f) Mongin, O.; Schuwey, A.; Vallot, M.-A.; Gossauer, A. *Tetrahedron Lett*. **1999**, *40*, 8347−8350. (g) Cho, H. S.; Rhee, H.; Song, J. K.; Min, C.-K.; Takase, M.; Aratani, N.; Cho, S.; Osuka, A.; Joo, T.; Kim, D. *J. Am. Chem. Soc*. **2003**, *125*, 5849−5860. (h) Peng, X.; Aratani, N.; Takagi, A.; Matsumoto, T.; Kawai, T.; Hwang, I.-W.; Ahn, T. K.; Kim, D.; Osuka, A. *J. Am. Chem. Soc.* **2004**, *126*, 4468−4469.

(4) (a) Satake, A.; Kobuke, Y. *Tetrahedron* **2005**, *61*, 13−41. (b) Chi, X.; Guerin, A. J.; Haycock, R. A.; Hunter, C. A.; Sarson, L. D. *Chem. Commun.* **1995**, 2567−2569. (c) Drain, C. M.; Russell, K. C.; Lehn, J.-M. *Chem. Commun.* **1996**, 337−338. (d) Knapp, S.; Vasudevan, J.; Emge, T. J.; Arison, B. H.; Potenza, J. A.; Schugar, H. J. *Angew. Chem., Int. Ed.* **1998**, *37*, 2368−2370. (e) Rubtsov, I. V.; Kobuke, Y.; H. Miyaji, H.; Yoshihara, K. *Chem. Phys. Lett*. **1999**, *308*, 323−328. (f) Kuroda, Y.; Sugou, K.; Sasaki, K. *J. Am. Chem. Soc.* **2000**, *122*, 7833−7834. (g) Ikeda, C.; Nagahara, N.; Yoshioka, N.; Inoue, H. *New J. Chem.* **2000**, *24*, 897−902. (h) Tsuda, A.; Nakamura, T.; Sakamoto, S.; Yamaguchi, K.; Osuka, A. *Angew. Chem., Int. Ed.* **2002**, *41*, 2817−2821.

(5) (a) Takahashi, R.; Kobuke, Y. *J. Am. Chem. Soc.* **2003**, *125*, 2372−2373. (b) Ikeda, C.; Satake, A.; Kobuke, Y. *Org. Lett.* **2003**, *5*, 4935−4938. (c) Ohashi, A.; Satake, A.; Kobuke, Y. *Bull. Chem. Soc. Jpn.* **2004**, *77*, 365−374. (d) Kuramochi, Y.; Satake, A.; Kobuke, Y. *J. Am. Chem. Soc.* **2004**, *126*, 8668−8669.

(6) Kobuke, Y.; Miyaji, H. *J. Am. Chem. Soc.* **1994**, *116*, 4111−4112.

(7) Ogawa, K.; Kobuke, Y. *Angew. Chem., Int. Ed.* **2000**, *39*, 4070−4073.

(8) (a) Tabushi, I.; Sasaki, T. *Tetrahedron Lett.* **1982**, *23*, 1913−1916. (b) Tabushi, I.; Kugimiya, S.; Kinnaird, M. G.; Sasaki, T. *J. Am. Chem. Soc.* **1985**, *107*, 4192−4199.

(9) Tomohiro, Y.; Satake, A.; Kobuke, Y. *J. Org. Chem.* **2001**, *66*, 8442−8446.

ing Information). Purification was achieved by combining three kinds of chromatographies (basic alumina, silica gel, and gel permeation columns), and analytically pure free base gable porphyrin **1** was obtained in a 2.1% total yield.[5a]

From 600 MHz ^{1}H NMR measurement of this gable porphyrin **1**, three atropisomers were observed in a 1:2:1 statistical ratio. We examined the formation and isomerization barrier of atropisomers of bis(1-methylimidazolyl)-porphyrins. The steric hindrance between 1-methyl group of imidazolyl ring and β-protons of pyrrole rings caused an orientation of the imidazolyl group perpendicular to the porphyrin plane. The atropisomers were distinguished from different chemical shifts most clearly of the 1-methyl of imidazolyl group, induced by a ring current effect from the porphyrin plane. The rate of exchange between atropisomers was evaluated from NMR spectrum of free base gable porphyrin **1** in the temperature range 373−301 K. A plot of ln k versus $1/T$ (Figure S1) gave the activation energy $\Delta G^{\ddagger}_{298K}$ at 298 K of 71.1 kJ mol^{-1}. In the case of *m*-phenyl and *m*-*o*-fluoro-phenyl, rotational barriers were reported as 45 ± 5 kJ mol^{-1} at 210 K and 93.2 ± 1.3 kJ mol^{-1} at 298 K, respectively.[10] Further, in the case of *trans*-bis(1-methylimidazol-2-yl)-porphyrin, no coalescence was observed at temperatures lower than 373 K. Considering these points, gable porphyrin **1** might rotate not around the 1-methylimidazolyl sides, but around the phenyl ring sides. Relatively large activation energy $\Delta G^{\ddagger}$ of **1** compared to that of *m*-phenylporphyrin may come from slower rotational movement of bulky 3-porphyrinylphenyl substituent.

Zinc(II) Insertion into Gable Porphyrin. We adopted an acetate method to insert zinc(II) ion to imidazolylporphyrin under mild condition at room temperature. Zinc insertion converted free base porphyrin **1** quantitatively to the corresponding zinc complex **2**, which was spontaneously organized by complementary coordination of imidazolylporphyrinatozinc motif to give an assembly ***X***. The molecular size distribution of zinc gable porphyrin assembly ***X*** was analyzed by gel permeation chromatography (GPC) and was observed as an oligomeric mixture with a broad distribution of the molecular weight (Figure 1a). However, the elution curve was totally different from that of *meso-meso* coupled porphyrin dimer zinc complex, which showed a sharp peak at the exclusion limit (8 min) with long tailing, relevant to the formation of giant linear arrays.[7] The elution curve of ***X*** showed obviously longer elution time and distinct spikes at around 12.3 min, indicating the formation of oligomeric mixtures of smaller molecular weights along with an assembly of somewhat specific sizes. This result suggests a positive sign that the terminal imidazolyl group tends to find the zinc porphyrin counterpart at its own chain end leading to intramolecular cyclization rather than simply elongated zigzag chain.

Reorganization under High Dilution Conditions. In the previous report, we have developed a reorganization of the once formed structure to convert to other forms for *meso-meso* directly linked bis(imidazolyl)porphyrin.[7] This reorganization procedure is composed of cleavage and reformation processes of self-assembled porphyrin arrays by adding and removing coordinating solvents, respectively. During the process removing coordinating solvents, new porphyrin arrangements different from the original structures can be obtained by the choice of appropriate conditions. We applied this reorganization method to the zinc bis(imidazolyl) gable porphyrin assembly ***X***. To dominate the macrocyclization on reconstructing the coordination structure, we applied the high-dilution condition, which should favor the intramolecular process rather than the intermolecular oligomerization. The reorganization processes are as follows: (1) cleavage of the coordinate bond and dilution; the assembly ***X*** was dissolved in 5 μM of $CHCl_3$/methanol = 7/3 (v/v); (2) further cleavage and dilution; methanol was added to make a 3.5 μM solution of $CHCl_3$/methanol = 1/1 (v/v); and (3) finally, the solvent was evaporated at 25 ± 1 °C. The GPC chart of the sample after the reorganization processes showed a dramatic change (Figure 1b).

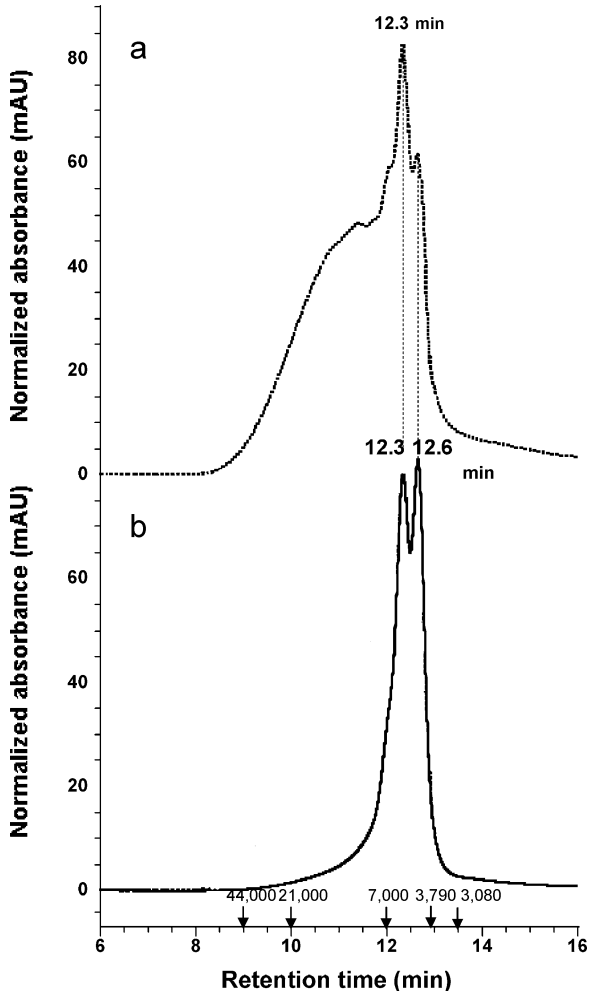

FIGURE 1. Gel permeation chromatograms for the assemblies ***X*** (a) and ***Y*** (b) with a column exclusion volume of 7×10^4 Da. The curves were normalized at the peak of 12.3 min. Each eluent is chloroform and 150 μM solutions were injected. The elution curve for ***X*** is shifted upward for clear comparison. Arrows along the *X*-axis indicate molecular weights of polystyrene standards.

In the reorganized sample ***Y***, the part due to larger molecular weights was eliminated almost completely and the peaks converged to two predominant peaks corresponding to the two spike peaks originally existing at the

(10) Crossley, M. J.; Field, L. D.; Forster, A. J.; Harding, M. M.; Sternhell, S. *J. Am. Chem. Soc.* **1987**, *109*, 341−348.

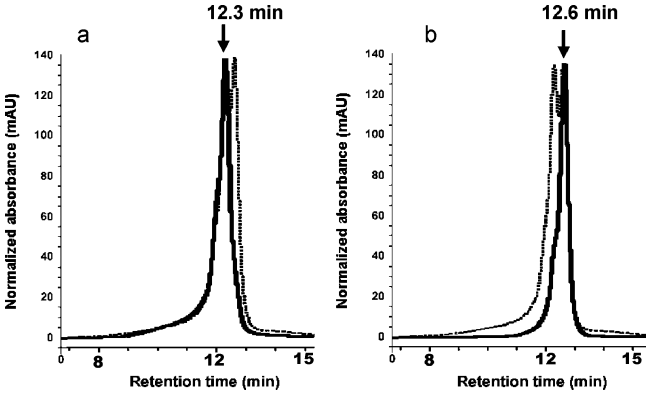

FIGURE 2. Gel permeation chromatograms (exclusion volume, 7 × 10^4 Da; eluent, chloroform) for assembly ***Y*** before separation (thin line) and for the isolated two components (bold lines) (a) **3** and (b) **4** after separation by using preparative gel permeation chromatography.

smallest molecular weight wing with smaller contributions. These converged peaks correspond to 7−9 porphyrins, if one applies a calibration curve obtained from linear *meso-meso* oligomers.[7] However, cyclic molecules are in general eluted later than the corresponding linear molecules because of smaller molecular sizes as shown not only from a theoretical consideration[11] but also from experimental results (e.g., poly(oxyethylene)s,[12a] polycarbazoles,[12b] and polystyrenes[12c]), and the observed peaks may correspond to the closed structure of hexagonal and related macrorings of gable porphyrins.

These two peak components were easily separated by using preparative GPC, employing toluene or benzene as the eluent. Each fraction was concentrated and injected again into the analytical column to confirm the clear separation and stability without any scrambling each other after the separation (Figure 2). In the following discussion, the first and the second isolated components are named **3** and **4**, respectively.

Probe Microscopy. Atomic force microscope (AFM) measurements of the assembly ***Y*** on flat mica substrate demonstrated the presence of round-shaped particles (Figure 3). Observation with further enlargement gave round-shaped particles of a uniform height (ca. 1.5 nm), which is characteristic of the height of the barrel-shaped macroring. The size, after correction of the radius curvature of the AFM probe (ca. 10 nm), provides the net diameter of the particles as a few nanometers. These particles are main components of the minimum size corresponding to the single molecule of the barrel-shaped macroring, although accompanied by larger circular spots presumably of their aggregates. The formation of these aggregates could not be avoided, because utilization of a further diluted solution caused disaggregated species of gable porphyrins in the deposition process. Since large linear arrays such as observed for *meso-meso* coupled porphyrin[7] could not be detected, the reorganization

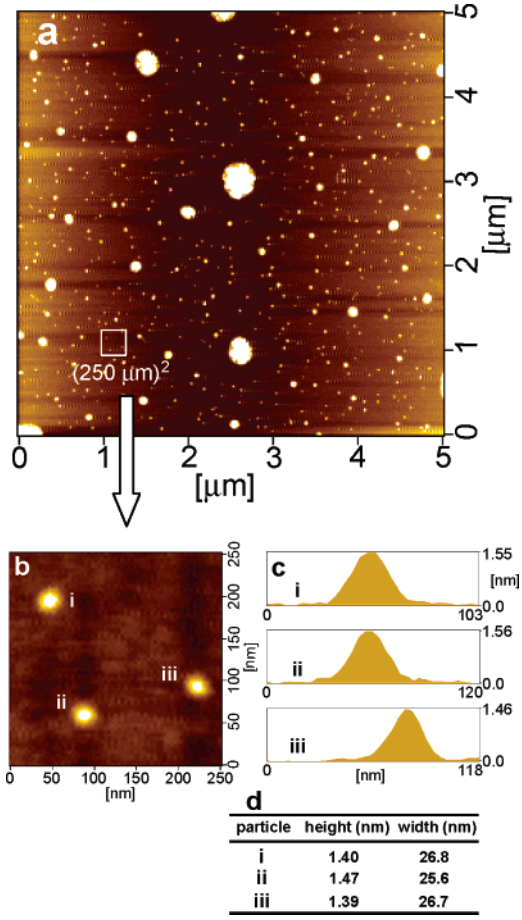

FIGURE 3. (a) AFM images of assembly ***Y*** (nearly 1:1 mixture of **3** and **4**) spin coated on mica substrate. (b) Enlarged results of AFM measurement for the area framed by a square in (a). (c) Cross-section profile of each particle appearing in (b). (d) Height and width of each particle. The widths were derived from half widths of the images without probe size correction.

processes converted completely the polymeric assemblies ***X*** to a mixture of macrorings ***Y***.

It should be noted that each component **3** and **4** is very stable both in solid and in solution states unless coordinating solvents are added. In AFM measurements, particles were observed similarly after 2 months of standing on the mica substrate, and observation on highly oriented pyrolytic graphite (HOPG) substrate gave also similar results (Figure 4). However, there was a tendency that particles on HOPG substrate were observed along the steps of the surface, which indicates a different particle distribution under different conditions.[13]

STM measurements on HOPG substrate were attempted for the sample ***Y***, whose uniform particles were confirmed by AFM measurements. Similar to the AFM images, many particles tended to locate along the steps of the HOPG surface in the STM measurements. Because particles of ***Y*** were not stable on repeated scanning by STM probe,[13a] we observed only a single molecular image of low resolution (Figure 5). Although the observed

(11) Skvortsov, A. M.; Gorbunov, A. A. *J. Chromatogr.* **1990**, *507*, 487−496.

(12) (a) Yu, G.-E.; Sinnathamby, P.; Prise, C.; Booth, C. *Chem. Commun.* **1996**, 31−32. (b) Zhang, Y.; Wada, T.; Sasabe, H. *Chem. Commun.* **1996**, 621−622. (c) Lepoittevin, B.; Dourges, M.-A.; Masure, M.; Hemery, P.; Baran, K.; Cramail, H. *Macromolecules* **2000**, *33*, 8218−8224.

(13) (a) Han, W.; Li, S.; Lindsay, S. M.; Gust, D.; Moore, T. A.; Moore, A. L. *Langmuir* **1996**, *12*, 5742−5744. (b) Milic, T. N.; Chi, N.; Yablon, D. G.; Flynn, G. W.; Batteas, J. D.; Drain, C. M. *Angew. Chem., Int. Ed.* **2002**, *41*, 2117−2119. (c) Yin, J.; Guo, Q.; Palmer, R. E.; Bampos, N.; Sanders, J. K. M. *J. Phys. Chem. B* **2003**, *107*, 209−216.

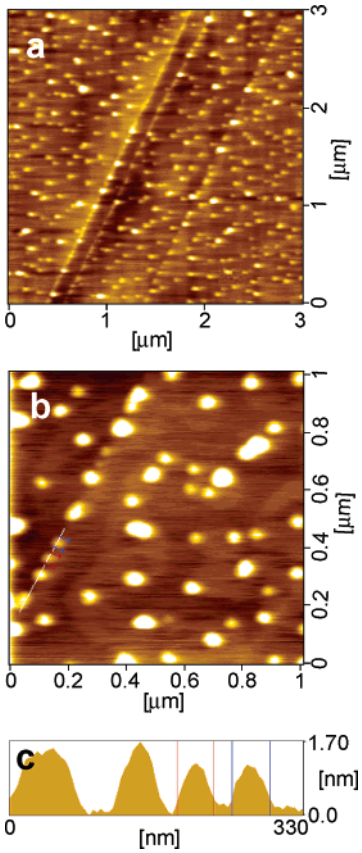

FIGURE 4. (a) AFM image of assembly ***Y*** spin coated on HOPG substrate. (b) Enlarged image of ***Y***. (c) Cross-section profile of particles along the step of HOPG substrate in (b).

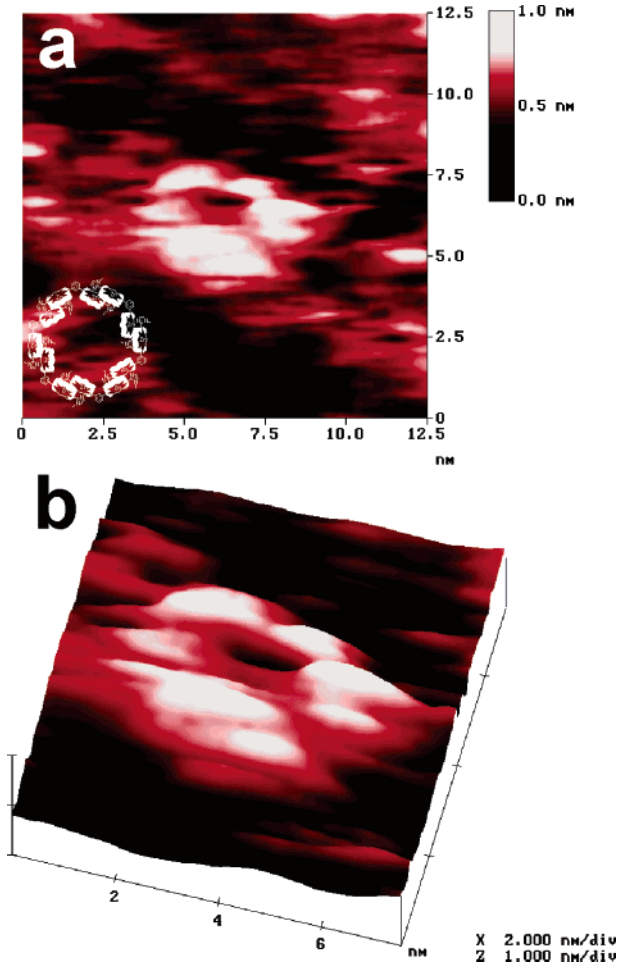

FIGURE 5. (a) STM image of ***Y*** spin coated on HOPG substrate. (b) Birds-eye view of image (a). Inset shows the schematic structure of hexameric gable porphyrin **3** drawn at the same scale.

molecular image was composed of disconnected gable porphyrins, this image was in good agreement with the size of the macroring of gable porphyrins.

Synchrotron Solution Small-Angle X-ray Scattering. Using the above probe microscopies, the macroring structure of gable porphyrins was suggested to exist on solid surface. Unfortunately, we could not determine the specific molecular weight by MALDI-TOF MS typically used for covalently linked organic compounds. All GPC fractions gave predominantly a monomer peak associated with a small dimer peak and trace higher oligomer ones. We finally applied small-angle X-ray scattering (SAXS) measurements for the isolated components, **3** and **4**, with a synchrotron radiation equipment. From SAXS measurements, we obtained information on (1) global size from the $q^2-\ln I(q)$ plot (Guinier plot) and (2) molecular shape information from $q-\ln I(q)$ plot, where q and $I(q)$ are scattering vectors in $Å^{-1}$, $q = (2\pi \sin \theta)/\lambda$, and scattering intensity, respectively.

The results of SAXS measurements for the first component **3** from GPC analysis with synchrotron radiation are as follows. The plot of scattering intensity vs square scattering vector (Guinier analysis) provided a radius of gyration (R_g) of 15.59 ± 0.34 Å for the predominant (98.0%) component (Figure 6a). This R_g value corresponds to diameters of 42 and 40 Å according to sphere and cylinder approximations, respectively. These values agree well with the estimation of ca. 41 Å for the outer diameter of the cyclic hexamer from molecular mechanics calculation with a universal force field (UNIVERSAL 1.02).[14] Furthermore, the particle size distribution was evaluated by the Funkuchen analysis, and the remaining 2% component gave R_g = 49 Å, which might correspond to particles of higher ordered aggregates. Similarly to **3**, SAXS measurements of the second component **4** from the GPC analysis were performed with synchrotron radiation. The Guinier analysis gave R_g = 11.12 ± 0.66 Å, and this R_g value corresponded to diameters of 29 Å according to the cylinder approximation (Figure 6b). Unfortunately, these SAXS results of **4** might be relatively less reliable compared to those of **3**, because the scattering intensity was relatively low.

To analyze further the SAXS results, we compared the experimental values with theoretical estimates by using molecular mechanics calculations by Cerius[2] with a universal force field[14] and a program package for SAXS analysis, CRYSOL.[15] The representative models are shown in Figure S2 (Supporting Information) with their theoretical R_g values. Three possible cyclic hexamers with C_2, C_3, and C_6 symmetries were considered in the calculation, and these isomers have similar R_g values of

(14) Rappé, A. K.; Casewit, C. J.; Colwell, K. S.; Goddard, W. A., III; Skiff, W. M. *J. Am. Chem. Soc.* **1992**, *114*, 10024−10035.
(15) Svergun, D. I.; Barberato, C.; Koch, M. H. J. *J. Appl. Crystallogr.* **1995**, *28*, 768−773.

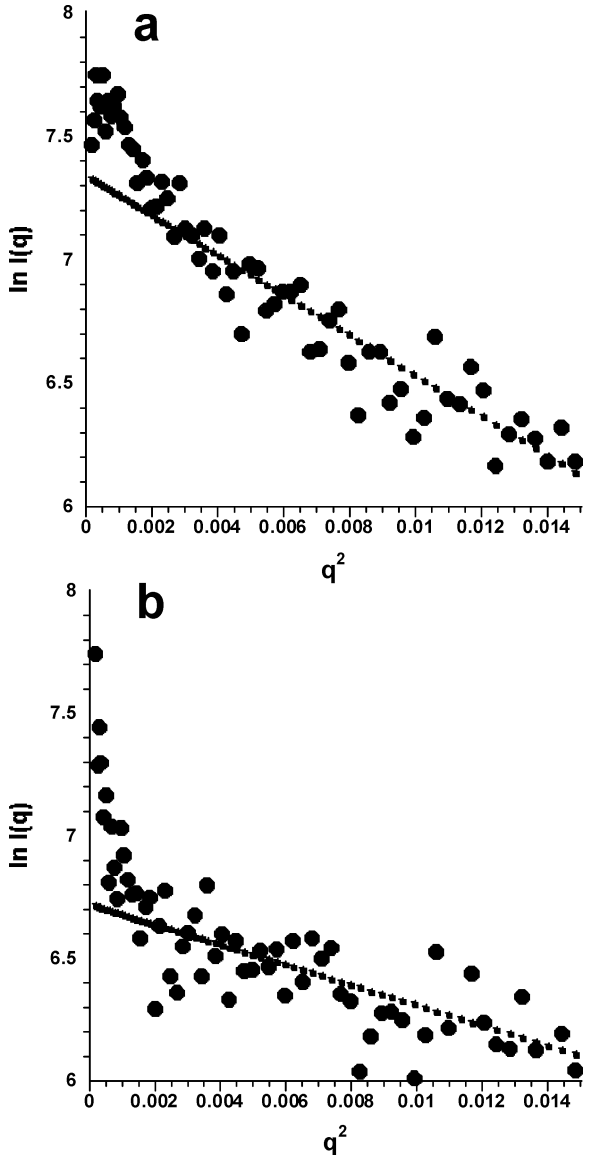

FIGURE 6. Gunier plot for SAXS measurements in methyl benzoate: (a) **3** (2.2 mg/mL) and (b) **4** (2.0 mg/mL), where q is the scattering vector in Å^{-1} and $I(q)$ is the scattering intensity.

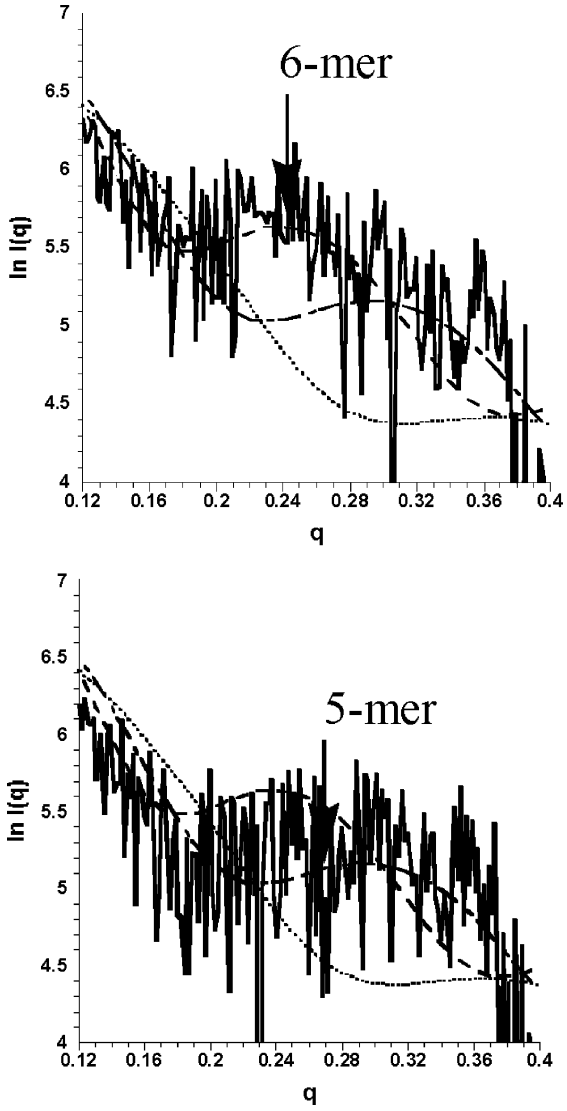

FIGURE 7. $q-\ln I(q)$ plot for SAXS measurements in methyl benzoate: (a) **3** (2.2 mg/mL) and (b) **4** (2.0 mg/mL) (solid curves). The theoretical curves for the cyclic hexamer, pentamer, and tetramer are indicated as broken, dash−dotted, and dotted lines, respectively.

16.54, 16.14, and 16.67 Å, respectively. The R_g values for the cyclic pentamer and tetramer gave 13.52 and 10.55 Å, respectively. The obtained R_g value for **3** is between the cyclic hexamer and cyclic pentamer, and that for **4** is between the cyclic pentamer and cyclic tetramer. It should be noted that linear arrays have R_g values distinctly larger than those of the corresponding cyclic arrays, 28.34, 23.76, and 19.43 Å for the linear hexamer, pentamer, and tetramer, respectively. Combining these results with GPC and reorganization behaviors, **3** and **4** may best be assigned as a cyclic hexamer and a cyclic pentamer, respectively.

Furthermore, the scattering profile in a wide-angle region was compared with theoretical models. This region gives information about the molecular shape from $q-\ln I(q)$ plots.[16] Theoretical $q-\ln I(q)$ plot for the model structures are shown in Figure S3. The cyclic hexamers with C_6, C_3, and C_2 symmetries gave similar scattering profiles, and we could not distinguish among them as same as the R_g values. On the other hand, distinct differences were observed among the cyclic hexamer, cyclic pentamer, and cyclic tetramer, all with waved scattering profiles showing the first minimum peaks at 0.18, 0.23, and 0.30 Å^{-1}, respectively. It should be noteworthy that these waved scattering profiles were not observed for linear oligomers, which gave monotonic profiles. Therefore if we observe waved profiles for $q-\ln I(q)$ plots, it might be regarded as characteristics of the hollow cylinder structures.

As expected from Figure S3, the scattering profile in a wide-angle region for both **3** and **4** gave waved profiles characteristic for the hollow cylinder structure (Figure 7). The first minimum peak of **3** appeared at 0.17 Å^{-1} followed by a rise of the intensity. This scattering intensity plot was expressed by a theoretical calculation[15] best for the cyclic hexamer with a minimum at 0.18 Å^{-1}, in contrast to other cyclic oligomers, the minimum being

(16) Pickover, C. A.; Engelman, D. M. *Biopolymers* **1982**, *21*, 817−831.

0.23 and 0.30 Å^{-1} for the pentamer and tetramer, respectively (Figure 7a) We conclude therefore at this point that **3** is a hexameric macroring. In the case of **4**, scattering intensity was relatively low and the first minimum peak was observed around 0.18−0.26 Å^{-1} (Figure 7b). Because this value roughly corresponds to the cyclic pentamer, we tentatively assign that **4** is a pentameric macroring.[17]

Mechanism of Reorganization Process. Summarizing the results described above, we could explain the components generated during the reorganization and separation processes as shown in Scheme 2. The reorganization processes under high dilution conditions are considered to proceed as follows. The dissociated gable porphyrin tries to find the counterpart, assisted by the large association constant of slipped-cofacial motifs. The high dilution condition, however, makes it difficult to find the counterpart in an intermolecular fashion in the solution. The small linear oligomer thus formed can find the counterpart at the other terminal in its own assembly to satisfy mutually the demand of complementary coordination. The most stable macroring must be composed of a hexameric unit since the *m*-gable motif with an interporphyrin angle of 120° is accommodated without angle strain. A pentameric assembly is also expected to form under forced conditions of high dilution if the angle strain is shared by the components. The heptameric species may be produced less favorably considering that the dynamic process starts from the lower unit sizes in the reorganization in accord with the experimental observations. It is important to note that the peak at 12.3 min constantly exists even after the first zinc insertion reaction under concentrated conditions (Figure 1), and this component matches the idea of the most thermodynamically stable product. On the other hand, the peak at 12.6 min became one of the major components after the reorganization and must be forced to generate during the reorganization process under high dilution conditions.

Considering that (1) there are three atropisomers in the *m*-gable motif and (2) once paired, slipped-cofacial motifs are difficult to dissociate, the observed convergent change by the reorganization process is very interesting. It must be noted that atropisomers can find their own partners to lead to the formation of three geometrical isomers of different symmetries, *C2*, *C3* and *C6*, for the hexamer **3** without any steric strain (Figure S2). If steric strain is allowed for the formation of macrocycles, isomers resulting from *out* and *in* coordination modes are allowed. The latter possibility may be favored considering the fact that macrocyclic pentamer **4**, where only one symmetry-allowed product is expected, was obtained in a yield even competitive with the hexamer.

Absorption Spectra. In view of the C_2 symmetry of the porphyrin chromophore, it may be that the electronic transition moment in a series of imidazolylporphyrins runs in the *meso-meso* direction. In fact, UV−vis absorption spectra of proximal porphyrins caused a splitting of the Soret band region for both slipped-cofacial and phenylene-bridged motifs. In the case of the slipped-cofacial motif, the splitting of the Soret bands might be qualitatively explained by the exciton coupling theory.[18] When this theory is applied to the slipped-cofacial

SCHEME 2. Schematic Representation of Reorganization Process under High Dilution Conditions and Further Separation Process into Hexameric Macroring 3 and Pentameric Macroring 4 of Gable Porphyrins

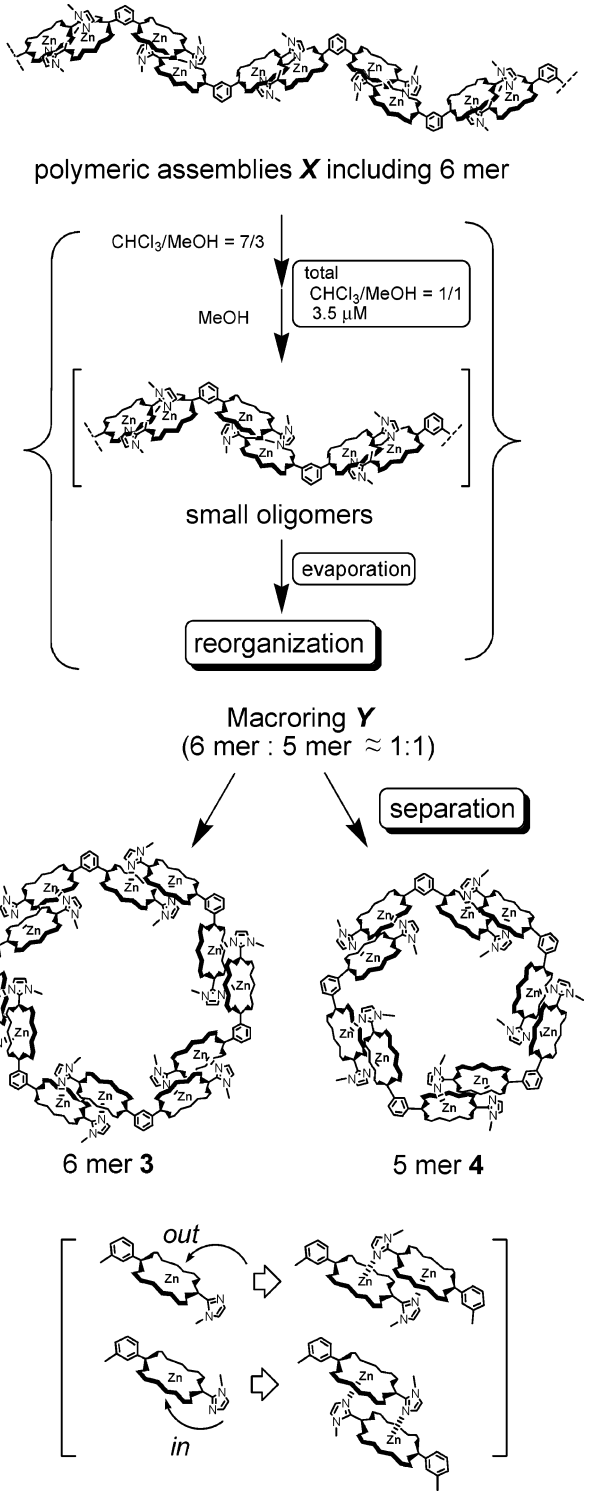

(17) We recently developed a method in which the complementary coordinated pair was connected covalently to each other by ring-closing metathesis reactions between *meso*-olefinic substituents.[5c] These macrocycles with *meso*-olefinic substituents, before the metathesis reaction, have shown behavior toward reorganization process and GPC analysis exactly the same as those of **3** and **4** and gave, after the metathesis, the exact molecular ion peaks corresponding to hexameric and pentameric gable porphyrins, respectively, by MALDI-TOF mass spectrometry.[5b]

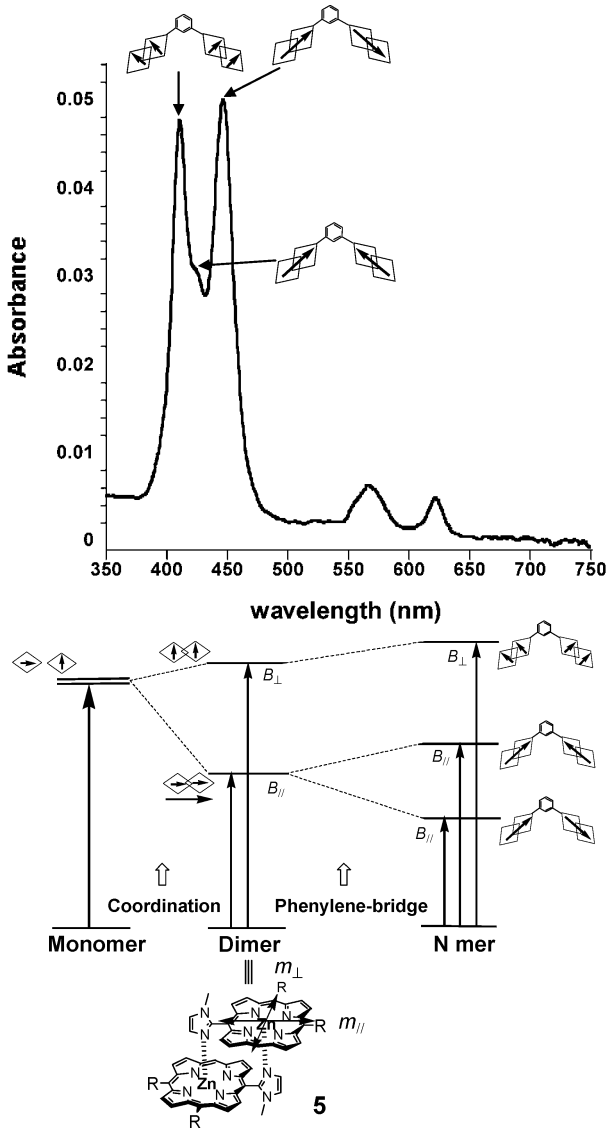

FIGURE 8. UV−vis absorption spectra of the macroring ***Y*** in benzene at room temperature and its exciton splitting modes.

arrangement, the degenerated Soret transitions, $B_{||}$ and $B_\perp$, in the monomeric unit are red- and blue-shifted depending on the head-to-tail and face-to-face orientations of the transition dipoles $m_{||}$ and $m_\perp$, respectively. In the case of the phenylene-bridged motif, the splitting of the Soret bands might be explained similarly. The red-shifted Soret transition $B_{||}$ might arise from the interaction between the transition dipoles $m_{||}$ on the head-to-tail orientation, and the other unperturbed Soret transition $B_\perp$ in the monomeric unit might be derived from both the head-to-head (tail-to-tail) orientations of the transition dipoles $m_{||}$ and the unperturbed transition dipoles $m_\perp$. UV−vis absorption spectrum of the macroring ***Y*** (hexamer:pentamer ≈1:1) solution gave a large splitting of the Soret bands and relatively unaffected Q-bands compared to the simple slipped-cofacial imidazolyl-zinc porphyrin dimer **5** (Figure 8).

This qualitative analysis of the absorption spectra indicates that electronic interactions between the closed porphyrins lead to perturbation of the Soret bands but not the Q-band absorptions when the pigments are linked to form the array. In the point-dipole approximation, the exciton coupling theory indicates that the interaction between chromophores should be inversely proportional to the cube of the interchromophoric distance and proportional to the square of the transition moments of the interacting chromophores. Thus, long-range exciton coupling in porphyrin arrays should only be detected for the Soret bands of higher oscillator strength and not for the Q-bands of a lower one, as is the case. In chloroform solution, UV−vis absorption spectra of hexamer **3** and pentamer **4** gave large splits of the Soret bands, 2073 and 2003 cm^{-1}, respectively. These correspond to the sum of each contribution of the splitting energy from slipped-cofacial and phenylene-bridged interactions,[18] 1310 and 775 cm^{-1}, respectively, the values of dimer **5** and of the monomeric bis-zinc gable porphyrin **2** (measured in the presence of excess 1-methylimidazole to dissociate the self-assembly).

Fluorescence Spectra. Fluorescence emission spectra of the macrorings (***Y***, **3**, and **4**) are similar to that of slipped-cofacial dimer **5**, reflecting the unperturbed Q-bands absorption. In contrast to the fact that a red-shifted and strongly quenched fluorescence was observed for artificial cofacial zinc dimers,[19] the macroring mixture ***Y*** showed fluorescence emission with nearly the same quantum yield (0.035) as those of tetraphenylporphyrinatozinc(II) (ZnTPP) (0.03)[20] as the reference. This fluorescence property ensures that the macrorings of gable porphyrins represent a good model for the artificial light-harvesting complex.

Conclusion

Combined evidence was consistent with the construction of porphyrin macrorings by interlocking 1,3-phenylene gable porphyrins by slipped-cofacial dimer formation without any protein matrices. This model must be a major milestone for further investigation to elucidate the mechanism of highly efficient light-harvesting in the natural photosynthetic system, as well as the facile strategy of such ring structure formation.

The principal finding of this study is the successful application of the reorganization methods that convert the once formed structure into desired structures, macroring arrays in this case. Oligomeric mixtures were converted almost completely to ring structures under high-dilution conditions by interlocking 1,3-phenylene gable porphyrins. This may be regarded as a typical advantage of supramolecular methodologies of structure formation. Various methods of application of such structural transformation may be designed. Not only the structure formation from only one component but also the addition of other components to the system must also be interesting.

The second important point is that the macroring arrays are candidates as light-harvesting antenna mim-

(18) Kasha, M.; Rawls, H. R.; El-Bayoumi, M. A. *Pure Appl. Chem.* **1965**, *11*, 371−392.

(19) Leighton, P.; Cowan, J. A.; Abraham, R. J.; Sanders, J. K. M. *J. Org. Chem.* **1988**, *53*, 733−740.

(20) Seybold, P. G.; Gouterman, M. *J. Mol. Spectrosc.* **1969**, *31*, 1−13.

ics. In general it is difficult to assemble donor molecules in a highly condensed state because of formation of undesired energy dissipation processes, e.g., concentration quenching, aggregation quenching, and nondirectional energy transfer, in homogeneous solution. However, the arrangement of chromophores in our macroring systems did not show any sign of fluorescence quenching by assembling in the ring structures, notwithstanding close interchromophoric distances, just as natural antenna chlorophyll molecules do. These findings must be correlated with the relation between the structure and function as seen in the natural light-harvesting systems. Elucidation of photophysical properties, especially energy migrating processes, will soon be reported.[21]

A further arrangement of ring components into a two-dimensional matrix such as a thylakoid membrane will be interesting, and the introduction of energy accepting units in the central cavity will also be of utmost importance. These challenges along with construction of novel macroring analogues are under active investigation in our laboratory. Our applications by learning plenty from nature must be beyond the natural systems and applicable for nanoscaled molecular devices in near future.

Experimental Section

Characterization of Porphyrin Supramolecules. AFM measurements were performed with Si tips (351 kHz, 42 N/m) for DFM (dynamic force mode) and tapping mode. Mica and highly oriented pyrolytic graphite (HOPG) were used as substrates. Typically, a 10 μM solution of assembly ***Y*** in chloroform or benzene was freshly prepared. A droplet of 1 μL of solution of ***Y*** was deposited on the substrate and spun at ca. 2,000 rpm for 10 s. An additional droplet of 4 μL of solution of ***Y*** was deposited on the substrate and spun at ca. 3,000 rpm for 10 s. The substrate was sprayed with nitrogen gas for 1 min and dried. Typical AFM parameters were as follows: rate of amplitude attenuation = −0.314 to −0.063; integral gain = 0.2273 to 0.8000; proportional gain = 0.0415 to 0.4980; scanning area = 5,000 to 175 nm; scanning frequency = 1.00 to 1.75 Hz.

STM measurements were performed with PtIr (80/20) tips. Measurements of ***Y*** on HOPG substrate were performed after verification of uniform particle images by preliminary AFM measurements. Typical STM parameters were as follows: gain = 10^{10} V/A for the high current mode, 10^{11} V/A for the low current mode; filter = 4.0 kHz; tip velocity = 0.201 to 0.155 μm/s; current set point = 500.0 to 3.00 pA; integral gain = 0.4000 to 1.0000; proportional gain = 0.3500 to 1.0000; bias = −2,000 to 2,000 mV; scanning area = 100 to 10 nm; scanning rate = 4.07 to 7.77 Hz.

Synchrotron SAXS measurements were performed by using synchrotron radiation at the solution scattering station (SAXES camera) installed at BL-10C, the Photon Factory, Tsukuba, Japan.[22]

Acknowledgment. We thank Prof. M. Kataoka and his laboratory members for technical assistance and helpful discussions with the SAXS measurements. This work was supported by CREST (Core Research for Evolutional Science and Technology) of the Japan Science and Technology Corporation (JST).

Supporting Information Available: Experimental details for synthesis of dipyrromethanes and porphyrins, Eyring plot for variable temperature NMR, Guinier plot for synchrotron SAXS, theoretical calculations, and other experimental conditions. This material is available free of charge via the Internet at http://pubs.acs.org.

JO047923N

(21) Hwang, I.-W.; Ko, D. M.; Ahn, T. K.; Kim, D.-H.; Ito, F.; Ishibashi, Y.; Khan, S. R.; Nagasawa, Y.; Miyasaka, H.; Ikeda, C.; Takahashi, R.; Ogawa, K.; Satake, A.; Kobuke, Y. Submitted for publication.

(22) Ueki, T.; Hiragi, Y.; Kataoka, M.; Inoko, Y.; Amemiya, Y.; Izumi, Y.; Tagawa, H.; Muroga, Y. *Biophys. Chem.* **1985**, *23*, 115−124.